

# Generation of Antitumor T Cells For Adoptive Cell Therapy With Artificial Antigen Presenting Cells

Bishwas Shrestha,\* Yongliang Zhang,\* Bin Yu,\* Gongbo Li,\* Justin C. Boucher,\*  
Nolan J. Beatty,\* Ho-Chien Tsai,† Xuefeng Wang,‡ Asmita Mishra,§  
Kendra Sweet,|| Jeffrey E. Lancet,|| Linda Kelley,¶ and Marco L. Davila\*§¶

**Summary:** Adoptive cell therapy with ex vivo expanded tumor infiltrating lymphocytes or gene engineering T cells expressing chimeric antigen receptors (CAR) is a promising treatment for cancer patients. This production utilizes T-cell activation and transduction with activation beads and RetroNectin, respectively. However, the high cost of production is an obstacle for the broad clinical application of novel immunotherapeutic cell products. To facilitate production we refined our approach by using artificial antigen presenting cells (aAPCs) with receptors that ligate CD3, CD28, and the CD137 ligand (CD137L or 41BBL), as well as express the heparin binding domain (HBD), which binds virus for gene-transfer. We have used these aAPC for ex vivo gene engineering and expansion of tumor infiltrating lymphocytes and CAR T cells. We found that aAPCs can support efficacious T-cell expansion and transduction. Moreover, aAPCs expanded T cells exhibit higher production of IFN- $\gamma$  and lower traits of T-cell exhaustion compared with bead expanded T cells. Our results suggest that aAPC provide a more physiological stimulus for T-cell activation than beads that persistently ligate T cells. The use of a renewable cell line to replace 2 critical reagents (beads and retroectin) for CAR T-cell production can significantly reduce the cost of production and make these therapies more accessible to patients.

**Key Words:** artificial antigen presenting cells, CAR T cells, adoptive T-cell therapy

(*J Immunother* 2020;43:79–88)

Cancer immunotherapy is a rapidly expanding area of research and clinical practice. Adoptive transfer of chimeric antigen receptor (CAR) T cells and tumor infiltrating lymphocytes (TILs) or marrow infiltrating lymphocytes (MILs) are promising strategies.<sup>1–4</sup> CD19-targeted CAR T cells for patients with B-cell acute lymphoblastic (B-ALL) or

diffusion large B-cell lymphoma generate efficacious response leading to their recent regulatory approval for patients in the United States and Europe.<sup>5,6</sup> Adoptive cell therapy with TILs has also exhibited long-lasting complete responses in patients with treatment-refractory melanoma.<sup>7,8</sup> MILs harvested from marrow of patients showed antitumor immunity and could be beneficial for solid tumors.<sup>4</sup> However, T-cell production methods used for CAR T cells, TILs, and MILs rely on protocols developed up to a decade ago, showing there is a need for further research to optimize antitumor T-cell production. In addition, the cost of the commercial CAR T-cell therapies is high with the production being one component for this high price. Therefore, we developed renewable artificial antigen presenting cells (aAPCs) to optimize antitumor T-cell function, as well as reduce costs.

Several groups have investigated aAPC to activate and/or expand T cells, or even modulate effector T-cell functions.<sup>9–11</sup> Butler et al<sup>10</sup> used K562 aAPCs expressing CD80 and CD83 to expand MART-1-specific T cells reactive against melanoma. While Maus et al<sup>12</sup> developed aAPC that expressed CD137 ligand (CD137L/41BBL) to ligate CD137 on T cells and also expressed CD32 to bind anti-CD3 and anti-CD28 antibodies for T-cell stimulation. RetroNectin is a common extracellular matrix fibronectin protein that has several cell and protein binding functions, and is commonly used to support transduction of T cells with CARs.<sup>13–15</sup> The common site for virus binding in RetroNectin is the heparin II domain.<sup>16</sup> Studies have shown the importance of the heparin II binding domain (HBD) in aiding gene transduction.<sup>15,17</sup> This led us to hypothesize that HBD domain can be used in aAPCs for gene transduction of CAR T cells.

In this study, we developed cell-based aAPCs expressing anti-CD3 and anti-CD28 single chain variable fragment (scFv) in combination with CD137L. After comparative studies of polyclonal T cells stimulated with CD3/28/137L aAPCs, and beads, we observed that aAPCs expanded CD8 T cells were less exhausted. Furthermore, when we modified the aAPC to also express the HBD they supported efficient gene transfer and the production of CAR T cells, which was equivalent to beads and was also scalable. Our reports demonstrate a strategy for optimization, both in terms of function and cost, of ex vivo antitumor T-cell production.

## MATERIALS AND METHODS

### Peripheral Blood Mononuclear Cells (PBMCs)

PBMCs from normal donors were obtained from buffy coats purchased from All Cells LLC (Emeryville, CA). MILs were isolated from bone marrow (BM) collected from patients at the Moffitt Cancer Center. The protocol used to

Received for publication June 27, 2019; accepted September 23, 2019. From the Departments of \*Clinical Science; †Biostatistics and Bioinformatics; §Blood & Marrow Transplant and Cellular Immunotherapy; ||Malignant Hematology Department; ¶Cellular Therapy Facility, H. Lee Moffitt Cancer Center and Research Institute; and ‡Morsani College of Medicine, University of South Florida, Tampa, FL.

B.S. and Y.Z. contributed equally.

Reprints: Marco L. Davila, H. Lee Moffitt Cancer Center and Research Institute, Tampa, FL 33612 (e-mail: marco.davila@moffitt.org).

Supplemental Digital Content is available for this article. Direct URL citations appear in the printed text and are provided in the HTML and PDF versions of this article on the journal's website, www.immunotherapy-journal.com.

Copyright © 2019 The Author(s). Published by Wolters Kluwer Health, Inc. This is an open-access article distributed under the terms of the Creative Commons Attribution-Non Commercial-No Derivatives License 4.0 (CCBY-NC-ND), where it is permissible to download and share the work provided it is properly cited. The work cannot be changed in any way or used commercially without permission from the journal.

collect patient samples was reviewed and approved by an Institutional Review Board at the H. Lee Moffitt Cancer Center and Research Institute. All patients provided written informed consent.

### Cell Lines

NIH/3T3, Chinese hamster ovary (CHO), and K562 cells were maintained in our laboratory and purchased from ATCC (Manassas, VA). Jurkat reporter cell lines were bought from Signosis Inc. (Santa Clara, CA). Cell lines were authenticated by short tandem repeats profile and inter cell species contamination test from IDEXX BioResearch (Columbia, MO). Complete medium for 3T3 cells and K562 contains DMEM supplemented with L-glutamine, penicillin/streptomycin and 10% fetal bovine serum. The medium for CHO is ATCC-formulated F-12K medium supplemented with 10% fetal bovine, L-glutamine, and penicillin/streptomycin. All media and supplements were bought from Thermo Fisher Scientific (Waltham, MA).

### Genetic Constructs and Cell-based aAPCs

The SFG retroviral construct was used for all constructs. SFG was modified to include an antihuman CD3 scFv including a GFP reporter and antihuman CD28 scFv containing a mCherry reporter, CD137L, and the HBD.<sup>18</sup> The CD3 and CD28 scFv constructs were linked with a CD8 $\alpha$  hinge and transmembrane domain followed by glycine/serine linker and GFP or mCherry respectively. SFG-HBD included 2 copies of the HBD in the extracellular compartment followed by a cerulean reporter in the intracellular domain. A Calcium Phosphate Transfection Kit (Promega, Madison, WI) was used to transfect retroviral construct into H29 packaging cells. Retroviral supernatants were harvested 4–5 days after transfection as described.<sup>19</sup> All 3T3, CHO, and K562 cells were transduced separately with retroviral supernatants to express CD3, CD28 scFv, and/or CD137L or HBD to create aAPCs. Transduced cells were sorted based on viability and fluorescence protein expression using a cell sorter BD FACSAria (BD Biosciences, San Jose, CA) at the Flow Cytometry Core Facility. Sorted aAPCs were expanded and cryopreserved; these cells were thawed and irradiated prior to use. The hCD19 CARs and hCD33 CARs paired with CD3 $\zeta$  and 41BB costimulatory domain was synthesized by Genewiz (South Plainfield, NJ) has been described previously.<sup>20</sup>

### Generation of h19BBz and hCD33BBz CAR T Cells

h19BBz or hCD33BBz CAR T cells were harvested, transduced, and formulated as previously described.<sup>19–21</sup> Briefly, PBMCs were isolated from the apheresis product of healthy donors by density gradient centrifugation with Ficoll plaque (Sigma-Aldrich, St Louis). T cells were isolated using a negative selection T-cell kit (StemCells Inc., Cambridge, MA). T cells were activated with either anti-CD3 and anti-CD28 (CD3/28) beads (Thermo Fisher Scientific) or K562 CD3/28 aAPCs and transduced with gamma retrovirus virus containing hCD19BBz or hCD33-BBz CAR and cultured in complete medium containing RPMI, L-glutamine, penicillin/streptomycin and 10% fetal bovine serum. Gamma retro virus was produced as described.<sup>19</sup> After 7 days of transduction, CAR T cells were expanded in G-REX flasks (WilsonWolf, St. Paul, MN) with beads or irradiated K562 CD3/28/137L aAPCs (10 Gy) for an additional 7 days. Transduction efficiency

was estimated as percentage of GFP<sup>+</sup> or mcherry<sup>+</sup> live cells as detected by a flow cytometer. Using a XRAD 160 irradiator (Precision X-ray Inc., N.Branford, CT), aAPCs were irradiated with 10 Gy at settings of 6.5 Gy/min.

### Flow Cytometry

The following antihuman antibodies with clones listed were obtained from BD Biosciences or ThermoFisher. Anti-B220 (HI30), anti-CD19 (SJ25-C1), anti-CD3 (UCH71), anti-CD4 (SK3), anti-CD8 (RPA-T8), anti-PD1 (eBioJ105), CD45RA (HI100), CD45RO (UCHL1), CCR7 (3D12), TIM3 (1D12), CTLA4 (14D3), anti-Thy1.1 (HIS51), anti-IFN- $\gamma$  (XMG1.2), CD137L (5F4, PE), and Live/dead Near-IR. Antibody staining was performed at 4°C with human Fc-block in MACS buffer with 0.5% BSA (Miltenyi Biotec Auburn, CA). Cells were washed twice and processed through a 5-laser BD LSRII or BD FACSymphony (BD Biosciences). For some experiments, countbright beads (Thermo Fisher Scientific) were used for cell quantification. T cells were defined as CD8 naive (CD3<sup>+</sup>CD8<sup>+</sup>CD45RA<sup>+</sup>CD45RO<sup>-</sup>) central memory T cells (T<sub>CM</sub>) with CD3<sup>+</sup>CD8<sup>+</sup>CD45RA<sup>-</sup>CD45RO<sup>+</sup>CCR7<sup>+</sup> and effector memory T cells (T<sub>EM</sub>) with CD3<sup>+</sup>CD8<sup>+</sup>CD45RA<sup>-</sup>CD45RO<sup>+</sup>CCR7<sup>-</sup>. For intracellular staining, 1 million transduced T cells were cocultured with 1 $\times$ 10<sup>5</sup> irradiated (30 Gy) 3T3-mCD19 cells for 4 hours in the presence of IL-2 with (for cytokines) or without (for antiapoptotic proteins) protein transport inhibitor (ThermoFisher). Cells were then treated using the Intracellular Fixation and Permeabilization Buffer Set (ThermoFisher) and stained following the manufacturer's protocol. Flow cytometry data were analyzed using FlowJo software (Tree Star).

### Cytotoxicity Assay

Cytotoxicity assays were run on an xCELLigence RTCA (Real Time Cell Analysis) instrument (ACEA Biosciences, San Diego, CA) according to the manufacturer's instructions. Briefly, 3T3-mCD19 cells or CHO-hCD33 were seeded overnight at 10,000 per well in an E-Plate 96 (ACEA Biosciences). CAR T cells were resuspended in fresh complete medium and added onto target cells at 100,000 cells per well at an E:T ratio of 10:1. Cell growth was monitored for a week.

### Metabolic Assay (Seahorse Bioanalyzer)

Cryopreserved healthy T cells expanded for 14 days with either K562 CD3/28/137L or beads CD3/28/137L were thawed and rested overnight. Freshly isolated T cells were used as a control. All groups of cells were activated with OKT3 overnight and CD8 T cells were isolated using EasySep Human CD8<sup>+</sup> T cells Isolation Kit (StemCells Inc., Cambridge, MA). Extracellular acidification rate (ECAR) and oxygen consumption rate (OCAR) was assessed with XF96 flux analyzer kit and Seahorse, Agilent per manufacture's instruction (Sea Horse Bioscience, Billerica, MA)

### Statistics

Means were compared using ordinary 1-way analysis of variance or 2-way analysis of variance followed by Tukey's test for multiple comparisons. \**P* < 0.05 was considered to be statistically significant. All statistical analyses were performed with Prism 6 software (Graphpad).

**RESULTS**

**K562 CD3/28/137L Efficiently Expand Health Donor Human T Cells**

To facilitate ex vivo generation of a large number of antitumor T cells, we developed cell-based artificial APC (aAPCs) by transducing K562 with gamma retrovirus encoding anti-CD3 and anti-CD28 scFv, as well as CD137L to enable stable expression of T-cell activation and costimulatory signals (Fig. 1A). Transduced K562 cells were enriched for CD3 scFv, CD28 scFv, and CD137L by fluorescent activated cell sorting (Fig. 1B).

To investigate the ability of aAPCs to support T-cell expansion we isolated T cells from healthy donor PBMCs (ALLcells) using a Human T-cell isolation Kit (Stem Cells Inc., Cambridge, MA) and cocultured with K562 aAPCs for 14 days in G-REX flasks (Wilson Wolf). K562 CD3/28/137L aAPCs supported 3.3-fold higher human CD3 T-cell expansion (mean, 348) compared with CD3/28/137L beads (mean, 106), and 3.5-fold higher than K562 CD3/28 aAPCs (mean, 99) and 1.6-fold higher than beads CD3/28 (mean, 220) (Fig. 2A). We did not detect any significant difference in naive CD8 T-cell expansion with either aAPCs or beads (Fig. 2B). In the process of ex vivo stimulation and expansion, T lymphocytes transition through progressive stages of differentiation that are characterized by a stepwise loss of functional and therapeutic potential. Thus, maintenance of stemness of T cells is critical for therapeutic efficiency.<sup>22,23</sup> We determined that K562 CD3/28/137L aAPCs efficaciously expanded T cells with memory features such as CD8 T<sub>EM</sub> (mean, 1321) and CD8 T<sub>CM</sub> (mean, 4407) compared with beads CD3/28/137L CD8 T<sub>EM</sub> (mean, 159) and CD8 T<sub>CM</sub> (mean, 1485) (Figs. 2C, D). Gating strategy of CD8 T subtypes is detailed in (Supplemental Fig. 1, Supplemental Digital Content 1, <http://links.lww.com/JIT/A548>). Exhaustion levels were not significantly different between T cells expanded with K562 CD3/28/137L aAPCs or beads

CD3/28/137L (Figs. 2E, F). Human CD4 T-cell fold expansion was highest with K562 CD3/28 aAPCs similar to CD3 cells (Supplemental Fig. 2, Supplemental Digital Content 1, <http://links.lww.com/JIT/A548>). Infusion of AAPCs is a safety concern but irradiated aAPCs cocultured with T cells are absent by 10 days demonstrating this is unlikely to be an obstacle for patient use (Supplemental Fig. 3, Supplemental Digital Content 1, <http://links.lww.com/JIT/A548>).

**K562 CD3/28/137L Support Expansion of T Cells From Acute Myeloid Leukemia (AML) Patients**

While expansion of T cells from healthy donor is efficacious with either activating beads or aAPCs, we wanted to evaluate how these technologies would support proliferation of T cells isolated from patients with AML, which has been difficult to achieve.<sup>24-26</sup> We isolated T cells from the BM of patients with AML. K562 CD3/28/137L aAPCs expanded T cells 3-fold higher than beads CD3/28/137L (mean, 344 vs. 114), as well as CD8 T<sub>EM</sub> 1.5-fold higher (mean, 993 vs. 658), and CD8 T<sub>CM</sub> subset 1.7-fold higher (mean, 593 vs. 354) (Fig. 3).

**K562 CD3/28/137L aAPCs Preserve Function of Stimulated T Cells**

While expression of exhaustion markers was similar we decided to investigate for evidence of functional exhaustion. Exhausted T cells exhibit decreased cytokine production and cytotoxic activity leading to poor immune response against tumors.<sup>27,28</sup> Therefore, we evaluated for exhaustion after using aAPC to expand TILs, which are more prone to exhaustion.<sup>29</sup> We isolated TILs from melanoma fragments of patients and cocultured with K562 CD3/28/137L aAPCs for 14 days followed by an overnight incubation with CD3/28 beads and Elispot to detect IFN- $\gamma$  production (Fig. 4A). K562 CD3/28/137L aAPCs showed high.

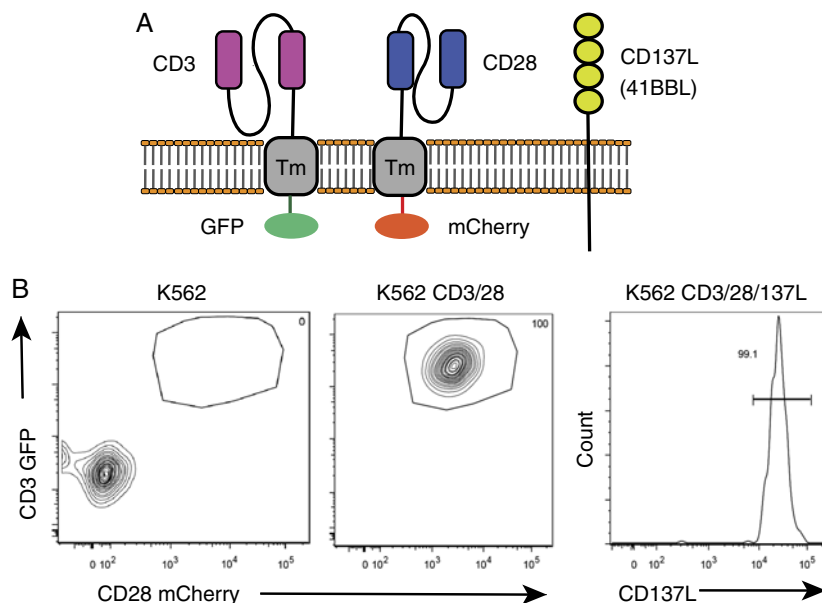


**FIGURE 1.** K562 aAPCs is transduced to express anti-CD3/28 scFv and CD137L 137L (41BBL). K562 cells were transduced with SFG retrovirus generated from H29 cells by transfection with calcium phosphate to induce stable expression of anti-CD3/28 and CD137L on K562. A, Schema of K562 cells expressing anti-CD3/28 and CD137L on cell surface tagged with fluorescent reporters. B, Flow plots depicting sorted K562 expressing CD3 scFv GFP, CD28 scFv mCherry, and CD137L stained with PE. Tm indicates transmembrane.

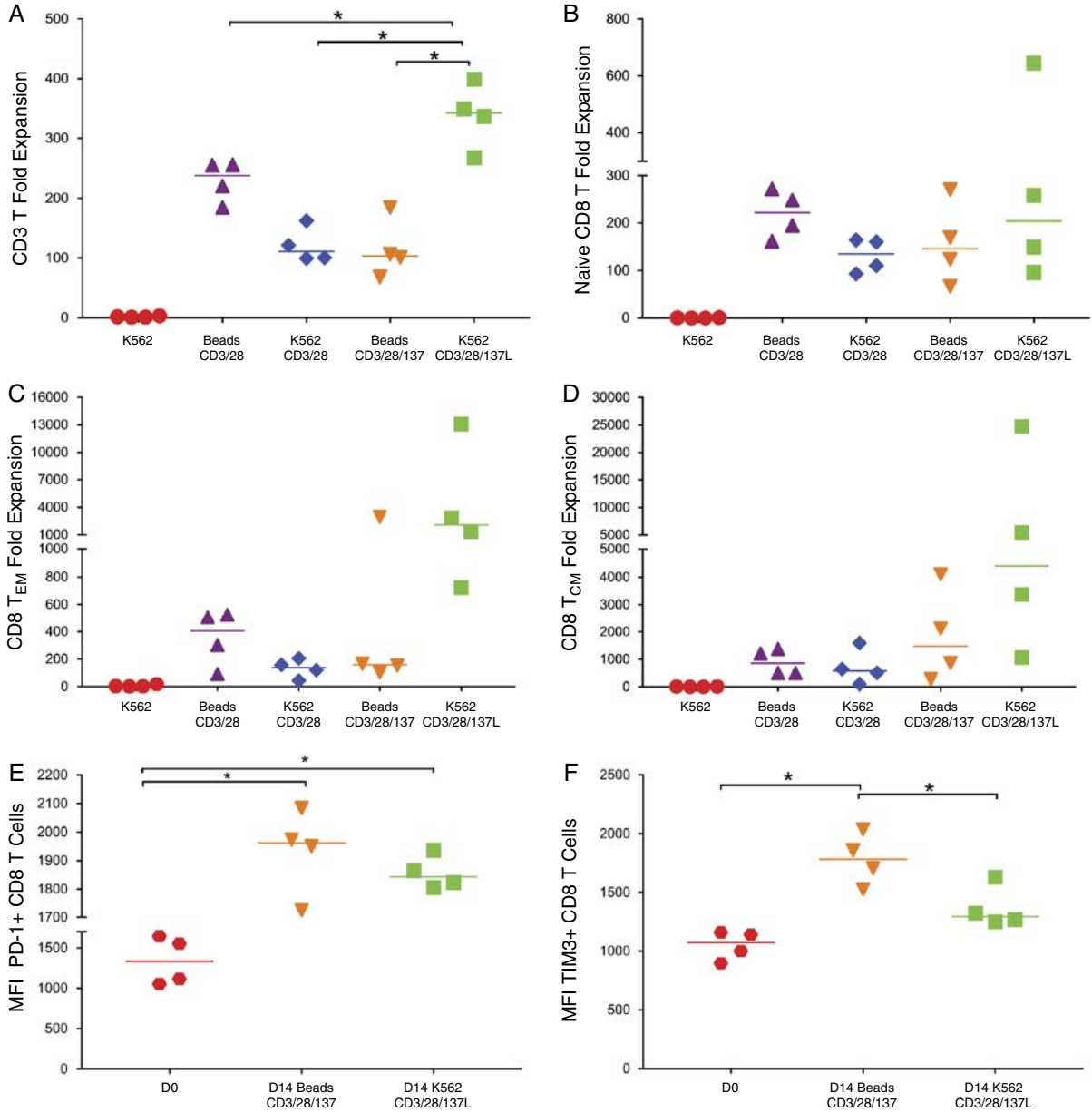


**FIGURE 2.** K562 CD3/28/137L efficiently expands healthy donor human T cells. T cells isolated from peripheral blood mononuclear cells of healthy donors were stimulated with aAPCs once (3:1 ratio) or beads (1:1) for 2 weeks in serum-free media in G-REX. T-cell expansion was measured by flow cytometer. A, CD3 T-cell fold expansion. B, Naive CD8 T cells CD45RO<sup>-</sup>CD45RA<sup>+</sup> fold expansion. C, CD8 T effector memory (CD45RO<sup>+</sup>CD45RA<sup>-</sup>CCR7<sup>-</sup>) fold expansion. D, CD8 T central memory (CD45RO<sup>+</sup>CD45RA<sup>-</sup>CCR7<sup>+</sup>) fold expansion. E, MFI PD-1<sup>+</sup> CD8 T cells. F, MFI TIM3<sup>+</sup> CD8 T cells. Each symbol in a group represents an individual donor. N = 4 per group. \*P ≤ 0.05 by 1-way analysis of variance Tukey test.

IFN- $\gamma$  producing cells compared with T cells activated with either K562 alone or K562 CD3/28 aAPCs. Furthermore, cells activated with CD3/28/137L K562 aAPCs also showed higher IFN- $\gamma$  production compared with CD3/28 K562 aAPCs as detected by flow cytometry (Fig. 4B). IFN- $\gamma$  production was highest in K562 alone stimulated group, but TILs cocultured with K562 alone did not expand demonstrating that these TILs are not stimulated. We also compared the expression of exhaustion markers by TILs activated with K562 aAPCs. T cells activated with K562 CD3/28/137L aAPCs had lower expression of PD-1 and

CTLA-4 (Fig. 4C) compared with K562 CD3/28 aAPCs suggesting that inclusion of CD137L reduces the induction of exhaustion despite repeated T-cell stimulation.

To investigate the differences between T cells activated with K562 CD3/28/137L and beads, we sought to explore the metabolic phenotype of expanded T cells. We measured the ECAR, a measure of intrinsic glycolysis and mitochondrial OCAR, an index of mitochondrial oxidative phosphorylation of CD8 T cells. K562 CD3/28/137L expanded CD8 T cells showed high ECAR and OCAR values compared with beads CD3/28/137L and unactivated

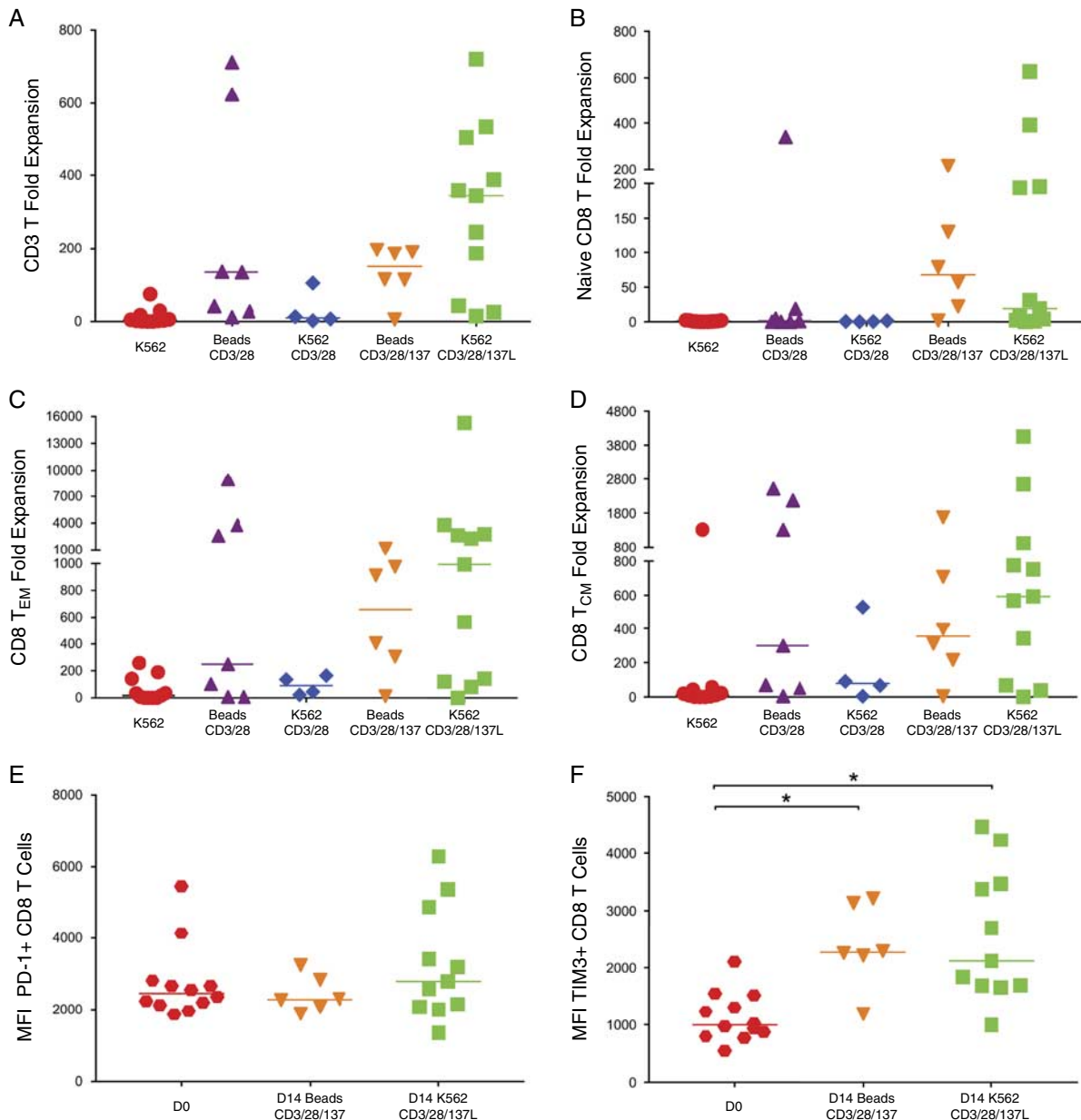


**FIGURE 3.** K562 CD3/28/137L efficiently expands T cells from AML patients. T cells isolated from bone marrow of AML patients were stimulated with indicated aAPCs once (3:1 ratio) or beads 1:1 for 2 weeks in serum-free media in G-REX. T-cell expansion was measured by a flow cytometer. A, CD3 T-cell fold expansion. B, Naive CD8 T cells CD45RO<sup>-</sup>CD45RA<sup>+</sup> fold expansion. C, CD8 T effector memory (CD45RO<sup>+</sup>CD45RA<sup>-</sup>CCR7<sup>-</sup>) fold expansion. D, CD8 T central memory (CD45RO<sup>+</sup>CD45RA<sup>-</sup>CCR7<sup>+</sup>) fold expansion. E, MFI PD1<sup>+</sup> CD8 T cells. F, MFI TIM3<sup>+</sup> CD8 T cells. Each symbol in a group represents an individual donor. N=4 to 11 per group. \**P*≤0.05 by 1-way analysis of variance Tukey test.

CD8 T cells (Fig. 4D). Therefore, CD8 T cells activated with K562 CD3/28/137L have a higher glycolytic phenotype concurrently with increased mitochondrial oxidation.

**Stable Expression of HBD in Cell-based aAPC Support Gene Transfer**

Cell-based aAPC support efficacious proliferation of T cells, which is required for viral transduction. However, we sought to modify the aAPC to also bind virus with the aim to enhance viral transduction. Therefore, we modified our cell-based aAPC to express the HBD, which is known

to bind virus and support gene transfer<sup>16,17</sup> (Fig. 5A). Design I has HBD between the CD3 or CD28 scFv and transmembrane domain. Design II has the CD3 or CD28 scFv between HBD and transmembrane domain. HBD is separated from the CD3 or CD28 scFv attached to its own transmembrane domain in the third design. Design III in which CD3 or CD28 scFv is expressed separate of the HBD displayed superior CAR gene transduction (Fig. 5A). We further demonstrated that the design III HBD supports cell-based aAPC CAR transduction regardless of the cell used to stimulate T cells. On the basis of these results we focused

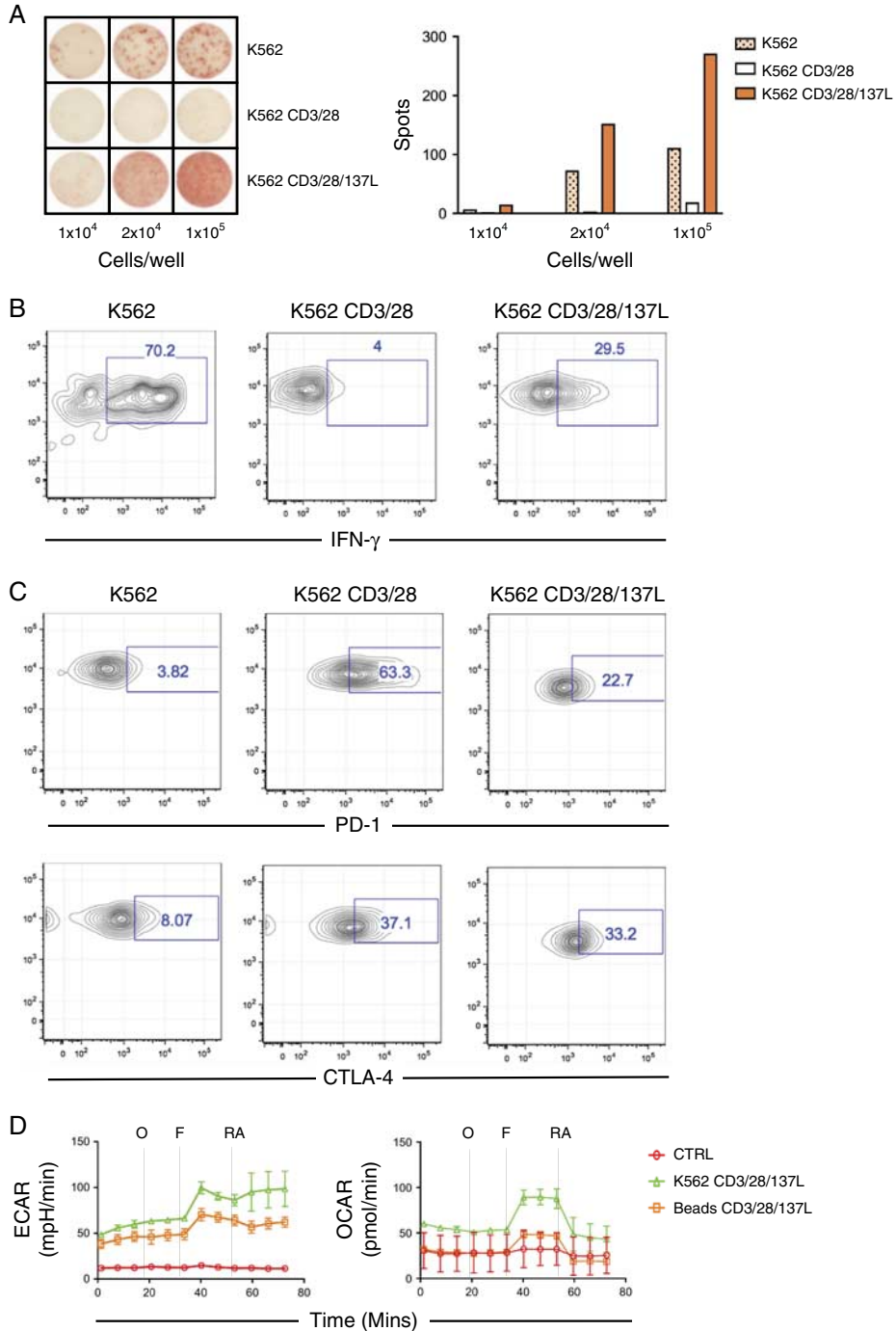


**FIGURE 4.** A–C, K562 CD3/28/137L aAPCs preserve function of stimulated T cells. Melanoma fragments were isolated from patients and digested. Tumor Infiltrating Lymphocytes (TILs) were then isolated and activated with aAPCs for 3 weeks and stimulated with beads for 14 hours. A, IFN- $\gamma$  producing T cells were read out by Elispot (L) and quantified (R). B, Intracellular staining of these TILs by Flow cytometry. C, TILs were stained with PD-1 and CTLA-4 antibodies and analyzed after gating on CD3 T cells. D, CD8 T cells from healthy donor T cells activated with indicated aAPCs or beads for 14 days were used for Seahorse XF Mito Stress test to calculate ECAR and OCAR. The control group (CTRL) is unactivated CD8 T cells. FCCP indicates carbonyl cyanide-4 (trifluoromethoxy) phenylhydrazone; O, oligomycin; RA, roteone antimycin.

only on design III for further experiments. We also demonstrated that both CHO and NIH/3T3 aAPCs (III) enhanced gene transduction compared with aAPCs lacking the HBD (Figs. 5B, C).

To assess the effect of CD3/28 HBD aAPCs on CAR T-cell proliferation and exhaustion we evaluated PD-1 and CTLA-4 expression. CD19-targeted CAR T cells were produced with CD3/28/HBD aAPCs without difference in

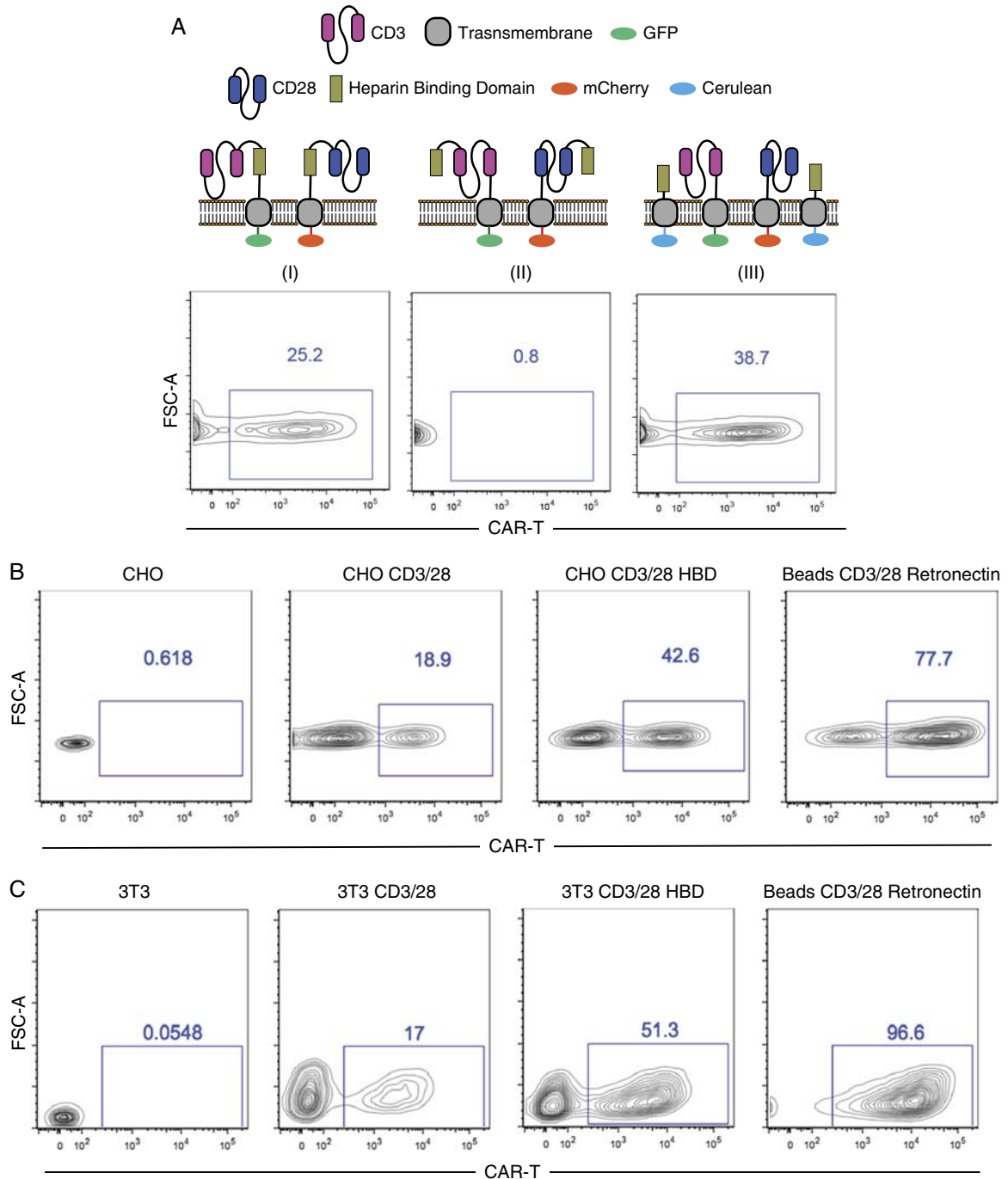


**FIGURE 5.** Stable expression of heparin binding domain (HBD) in cell-based aAPC support gene transfer. Cells were transduced with constructs of anti-CD3/28 and HBD (as shown of I, II, III) to generate anti-CD3/28/HBD aAPCs. HBD-mediated gene transduction were tested by coculture of indicated aAPC (I, II, III) with healthy donor T cells in the presence of CD19 CAR retrovirus. **A**, Transduction efficiency of CAR T with aAPC (I, II, III). For further productions we included aAPC design III since it was the most optimal. **B**, Comparison of transduction efficiency of CAR T (III) CHO CD3/28/HBD aAPCs with beads/retronectin. **C**, Comparison of transduction efficiency of CAR T with (III) 3T3 CD3/28/HBD aAPCs with beads/retronectin.

proliferation and expression of exhaustion markers compared with CD3/28 aAPCs, but lower proliferation and exhaustion when compared with beads (Fig. 6A). CD19-targeted CAR T cells stimulated with 3T3 aAPC alone showed lower levels of exhaustion by PD-1 and

CTLA-4 and no proliferation suggesting lack of antigen stimulation. In contrast, lower levels of PD-1 and CTLA-4 in CD19-targeted CAR T cells activated with CD3/28 aAPCs with or without HBD is not due to lack of antigen stimulation since they proliferate. To compare the cytotoxic

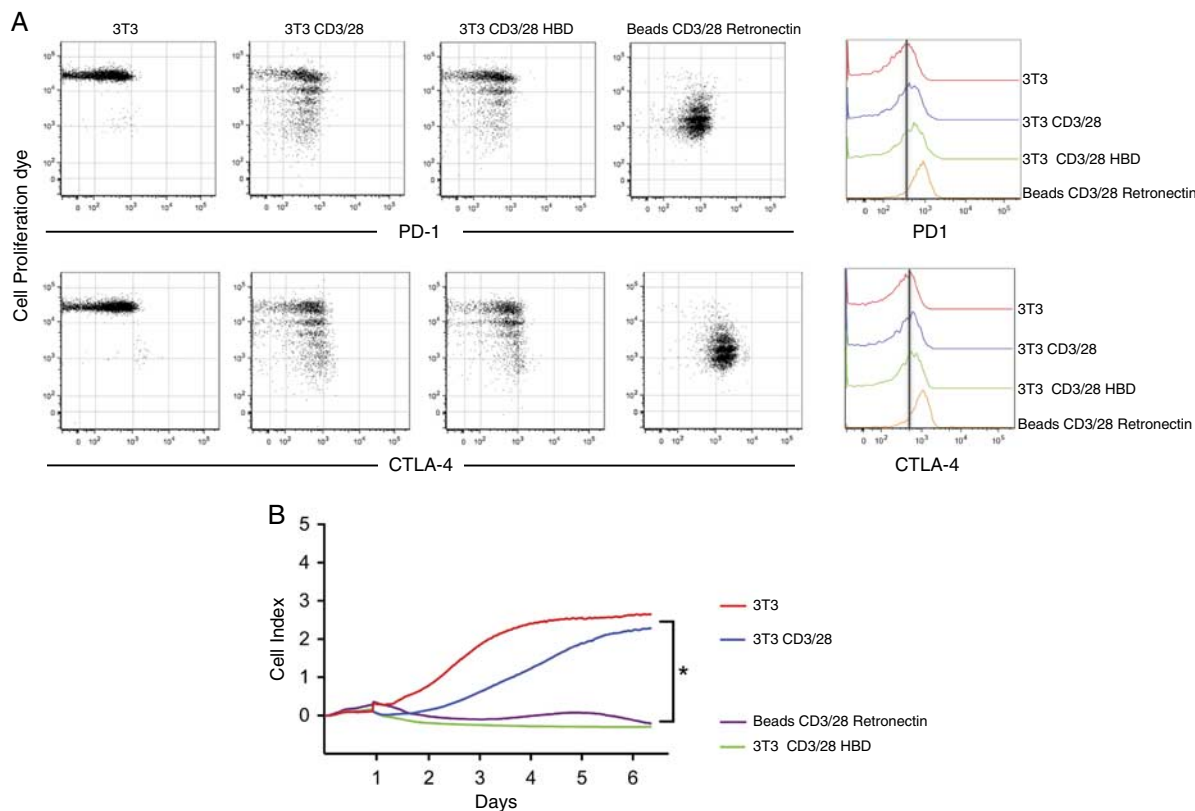


**FIGURE 6.** 3T3 CD3/28 HBD aAPCs reduce exhaustion markers, and support cytotoxic ability of CAR T cells. Human T cells isolated from healthy donor were stained with cell proliferating dye followed by activation with indicated aAPCs or beads and retroNectin and transduced with anti-CD19 CAR. After 7 days expansion, CAR T cells were stained with PD-1 and CTLA-4 antibody for analysis via flow cytometer or used to target CD19 cells for cytotoxicity. A, Proliferation of CAR T cells and exhaustion markers PD-1 and CTLA-4 gated on CAR T. Data are presented by dot plot (L) and histogram (R). B, Cell cytotoxicity assay measured by xCELLigence. 3T3 mouse CD19 target cells were incubated with anti-CD-19 CAR T cells activated with indicated aAPCs or beads in 10:1 ratio. \* $P < 0.05$  by 2-way analysis of variance Tukey test.

ability of CAR T cells activated with CD3/28 beads and RetroNectin to CD3/28 HBD aAPCs, we incubated CD19-targeted CAR T cells with target 3T3 cells expressing the CD19 antigen. There was no difference in the killing ability of CD19-targeted CAR T cells activated by beads CD3/28 and RetroNectin or CD3/28/HBD aAPC (Fig. 6B).

### aAPC Activate, Expand T Cells, and Support Cytotoxic Ability in a Scaled-up Production of CAR T Cells

We wanted to determine the feasibility of using cell-based aAPC for CAR T-cell production for patients with AMLs. Therefore, we determined if we could produce a dose of CAR T cells starting from a small number of T cells collected from a patient with AML. We used a CD33-targeted CAR construct that we recently developed<sup>20</sup> since CD33 is a promising target for AML.<sup>30–32</sup> We compared the immune phenotype, expansion, and cytotoxicity of CAR T cells activated with either cell-based or bead-based aAPC. We cocultured T cells, derived from the BM of an AML patient, with CD3/28/HBD aAPC for 7 days in a 6 well plate followed by CD3/28/137L aAPC for another 7 days in G-REX. For bead-based aAPC T cells were activated with CD3/28 beads for 7 days in a 6 well plate and then in G-REX with CD3/28/137L beads. There was no significant difference in transduction efficiency or CD4/CD8 immune

phenotypes between CD33-targeted CAR T cells produced with bead or cell-based aAPCs (Figs. 7A, B). However, there was a greater production of CD8 T<sub>EM</sub> (80%) and a greater yield of total CAR T cells ( $2 \times 10^8$  cells) (Figs. 7C, D). Anti-CD33 CAR T cells activated with either bead-based or cell-based aAPCs did not display differences in cytotoxicity of CD33<sup>+</sup> target cells (Fig. 7E), which demonstrates that cell-based aAPCs can also be used for clinical production of CAR T cells (Supplemental Fig. 4, Supplemental Digital Content 1, <http://links.lww.com/JIT/A548>).

## DISCUSSION

Expansion and transduction of autologous T cells requires the use of CD3/28 beads and RetroNectin. Here, we have developed renewable aAPCs with CD3/28 and HBD for expansion and transduction of CAR T cells. aAPCs were able to activate, expand, transduce, and enhance the cytotoxic ability of CAR T cells while attenuating exhaustion. We are making these human K562 cells GMP compliant.<sup>33</sup> We irradiate the aAPCs, which are also killed by CAR T cells during cell production. After in vitro expansion naive T cells will dynamically process into stem cell-like memory (T<sub>SCM</sub>), central memory (T<sub>CM</sub>), and effector memory (T<sub>EM</sub>) T cells upon TCR stimulation. Among these populations, T<sub>SCM</sub> possess superior persistence and antitumor effects in



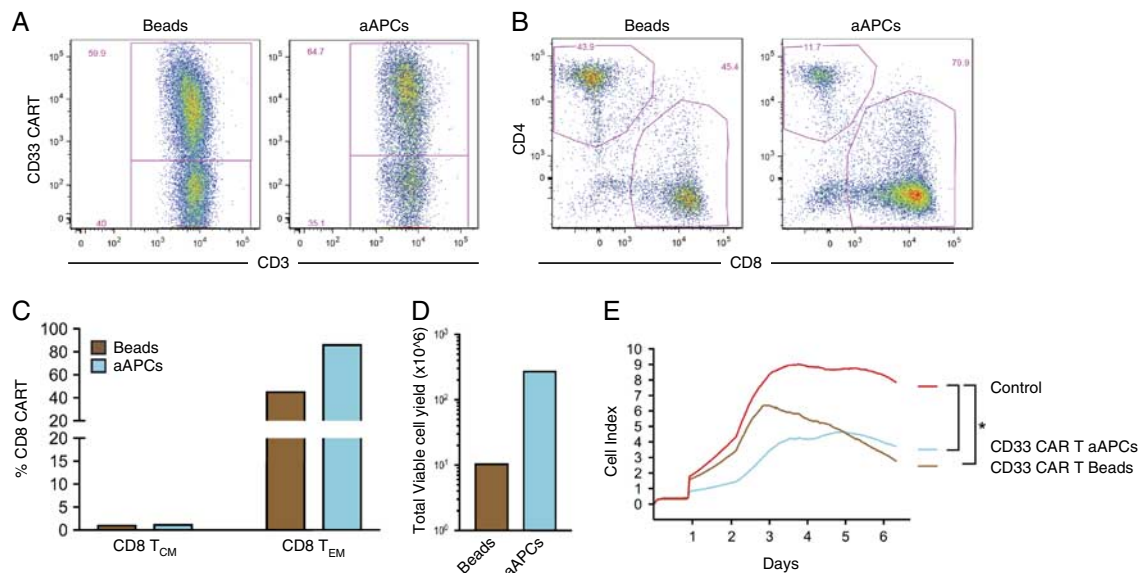


**FIGURE 7.** aAPCs activate, expand T cells, and enhance cytotoxic ability of a large scale preparation of CAR T cells. Human T cells isolated from peripheral blood mononuclear cells were transduced with CD33 CAR retrovirus and activated with CHO CD3/28/HBD or beads CD3/28 for 7 days. 1 million CAR T cells were then again expanded using K562 CD3/28/137L or CD3/28 beads in G-REX for 7 days. A, Transduction of CD33 CAR T. B, Phenotype of CAR T cells activated with aAPCs or beads. C, Percentage of CD8T<sub>CM</sub> and CD8T<sub>EM</sub>. D, Total cell yield in G-REX. E, Cell cytotoxicity assay measured by xCELLigence. CHO CD33 target cells were incubated with anti-CD33 CAR T cells produced with aAPCs or beads in a 10:1 ratio. Mock transduced T cells was used as a control. \**P* ≤ 0.05 by 2-way analysis of variance Tukey test.

multiple cancer immunotherapy models.<sup>22,23,34,35</sup> Since T cells lose the stemness and long-term survival potential during in vitro culture and stimulation, optimized strategies that generate and expand T<sub>SCM</sub> like cells are pivotal to the development of the next generation of highly effective T-cell-based immunotherapies. Although we did not see a significant difference in CD8T<sub>CM</sub> and CD8T<sub>EM</sub> between CD3/28/137L beads and aAPCs, there is a 2- to 3-fold expansion in these CD8 memory cells. This could be attributed to CD137L costimulation, which has been shown to support memory differentiation.<sup>36</sup>

Activation of T cells with CD3/28/137L aAPCs showed higher glycolysis and oxidation compared with bead activated T cells (Fig. 4D). This was expected because we see higher number of CD8 T effector cells (Figs. 2C, 3C) and these cells utilize more glucose and aerobic glycolysis.<sup>37</sup> Activation of T cells with aAPCs also showed higher percentage of memory CD8 T cells (Figs. 2D, 3D) and high rate of OCR for these cells (Fig. 4D). Kawalekar et al.<sup>38</sup> saw similar results where CAR T cells with 41BB/CD137L endodomain enhanced their oxidative phosphorylation which is characteristic of CD8 memory T cells.<sup>38</sup> Expansion of CD3 and CD8 T cells showed some differences from healthy patients (Fig. 2) compared with AML patients (Fig. 3). This was expected because T cells from AML patients have been shown to have abnormal phenotype and lack the ability to synapse effectively.<sup>39</sup>

It has been previously shown that HBD aids in gene transduction.<sup>15,17</sup> Here we designed CD3/28 aAPCs with HBD. We discovered that HBD needs to be in proximity with the trans membrane domain for gene transduction (Fig. 5). When HBD was away from the transmembrane and flanking to the side of CD3/28 scFv, HBD was not able to aid in transduction. While aAPCs with CD3/28 domain have been shown to activate T cells and increase production

of IFN- $\gamma$  from T cells, tumor-infiltrating lymphocytes from melanoma patients were not able to secrete IFN- $\gamma$  when activated with only CD3/28. This could be explained by exhaustion of T cells as seen by increased expression of CTLA-4 and PD-1 (Fig. 6B). Activating beads bind human T cells substantially and provide a strong continuous T-cell activation signal, which results in exhaustion.

Our findings suggest that CD3/28/137L aAPCs of clinical grade have therapeutic potential to generate large numbers of CAR T cells ex vivo for cancer immunotherapy. For effective remission of tumor, memory CD8 CAR T cells are desirable and can be obtained using the aAPC. Meanwhile, our optimized renewable aAPCs can greatly lower the cost of T-cell manufacture by replacing expensive reagents.

#### ACKNOWLEDGMENTS

The authors would like to thank the staff of the Flow Cytometry Core.

#### Conflicts of Interest/Financial Disclosures

This work was supported by funds from the H. Lee Moffitt Cancer Center and Research Institute as well as Celgene.

All authors have declared there are no financial conflicts of interest with regard to this work.

#### REFERENCES

- Rosenberg SA, Packard BS, Aebbersold PM, et al. Use of tumor-infiltrating lymphocytes and interleukin-2 in the immunotherapy of patients with metastatic melanoma. A preliminary report. *N Engl J Med.* 1988;319:1676–1680.
- Morgan RA, Dudley ME, Wunderlich JR, et al. Cancer regression in patients after transfer of genetically engineered lymphocytes. *Science.* 2006;314:126–129.

3. Porter DL, Levine BL, Kalos M, et al. Chimeric antigen receptor-modified T cells in chronic lymphoid leukemia. *N Engl J Med*. 2011;365:725–733.
4. Noonan KA, Huff CA, Davis J, et al. Adoptive transfer of activated marrow-infiltrating lymphocytes induces measurable antitumor immunity in the bone marrow in multiple myeloma. *Sci Transl Med*. 2015;7:288ra278.
5. Maude SL, Frey N, Shaw PA, et al. Chimeric antigen receptor T cells for sustained remissions in leukemia. *N Engl J Med*. 2014;371:1507–1517.
6. Neelapu SS, Locke FL, Bartlett NL, et al. Axicabtagene ciloleucel CAR T-cell therapy in refractory large B-cell lymphoma. *N Engl J Med*. 2017;377:2531–2544.
7. Besser MJ, Shapira-Frommer R, Schachter J. Tumor-infiltrating lymphocytes: clinical experience. *Cancer J*. 2015;21:465–469.
8. Andersen R, Donia M, Ellebaek E, et al. Long-lasting complete responses in patients with metastatic melanoma after adoptive cell therapy with tumor-infiltrating lymphocytes and an attenuated IL2 regimen. *Clin Cancer Res*. 2016;22:3734–3745.
9. Maus MV, Riley JL, Kwok WW, et al. HLA tetramer-based artificial antigen-presenting cells for stimulation of CD4+ T cells. *Clin Immunol*. 2003;106:16–22.
10. Butler MO, Lee JS, Ansen S, et al. Long-lived antitumor CD8+ lymphocytes for adoptive therapy generated using an artificial antigen-presenting cell. *Clin Cancer Res*. 2007;13:1857–1867.
11. Hasan AN, Kollen WJ, Trivedi D, et al. A panel of artificial APCs expressing prevalent HLA alleles permits generation of cytotoxic T cells specific for both dominant and subdominant viral epitopes for adoptive therapy. *J Immunol*. 2009;183:2837–2850.
12. Maus MV, Thomas AK, Leonard DG, et al. Ex vivo expansion of polyclonal and antigen-specific cytotoxic T lymphocytes by artificial APCs expressing ligands for the T-cell receptor, CD28 and 4-1BB. *Nat Biotechnol*. 2002;20:143–148.
13. Chono H, Yoshioka H, Ueno M, et al. Removal of inhibitory substances with recombinant fibronectin-CH-296 plates enhances the retroviral transduction efficiency of CD34(+)CD38(-) bone marrow cells. *J Biochem*. 2001;130:331–334.
14. Hanenberg H, Xiao XL, Dilloo D, et al. Colocalization of retrovirus and target cells on specific fibronectin fragments increases genetic transduction of mammalian cells. *Nat Med*. 1996;2:876–882.
15. Dodo K, Chono H, Saito N, et al. An efficient large-scale retroviral transduction method involving preloading the vector into a RetroNectin-coated bag with low-temperature shaking. *PLoS One*. 2014;9:e86275.
16. Moritz T, Dutt P, Xiao X, et al. Fibronectin improves transduction of reconstituting hematopoietic stem cells by retroviral vectors: evidence of direct viral binding to chymotryptic carboxy-terminal fragments. *Blood*. 1996;88:855–862.
17. Wu Z, Asokan A, Grieger JC, et al. Single amino acid changes can influence titer, heparin binding, and tissue tropism in different adeno-associated virus serotypes. *J Virol*. 2006;80:11393–11397.
18. Davila ML, Kloss CC, Gunset G, et al. CD19 CAR-targeted T cells induce long-term remission and B Cell Aplasia in an immunocompetent mouse model of B cell acute lymphoblastic leukemia. *PLoS One*. 2013;8:e61338.
19. Li G, Park K, Davila ML. Gammaretroviral production and T cell transduction to genetically retarget primary T cells against cancer. *Methods Mol Biol*. 2017;1514:111–118.
20. Li G, Boucher JC, Kotani H, et al. 4-1BB enhancement of CAR T function requires NF-kappaB and TRAFs. *JCI Insight*. 2018;3:1–18.
21. Ghosh A, Smith M, James SE, et al. Donor CD19 CAR T cells exert potent graft-versus-lymphoma activity with diminished graft-versus-host activity. *Nat Med*. 2017;23:242–249.
22. Gattinoni L, Klebanoff CA, Restifo NP. Paths to stemness: building the ultimate antitumor T cell. *Nat Rev Cancer*. 2012;12:671–684.
23. Gattinoni L, Lugli E, Ji Y, et al. A human memory T cell subset with stem cell-like properties. *Nat Med*. 2011;17:1290–1297.
24. Buggins AG, Milojkovic D, Arno MJ, et al. Microenvironment produced by acute myeloid leukemia cells prevents T cell activation and proliferation by inhibition of NF-kappaB, c-Myc, and pRb pathways. *J Immunol*. 2001;167:6021–6030.
25. Schuster SJ, Bishop MR, Tam C, et al. Global pivotal phase 2 trial of the Cd19-targeted therapy Ctl019 in adult patients with relapsed or refractory diffuse large B-cell lymphoma - an interim analysis. *Haematologica*. 2017;102:1–2.
26. Petersen CT, Hassan M, Morris AB, et al. Improving T-cell expansion and function for adoptive T-cell therapy using ex vivo treatment with PI3Kdelta inhibitors and VIP antagonists. *Blood Adv*. 2018;2:210–223.
27. Wherry EJ. T cell exhaustion. *Nat Immunol*. 2011;12:492–499.
28. Jiang Y, Li Y, Zhu B. T-cell exhaustion in the tumor microenvironment. *Cell Death Dis*. 2015;6:e1792.
29. Ahmadzadeh M, Johnson LA, Heemsker B, et al. Tumor antigen-specific CD8 T cells infiltrating the tumor express high levels of PD-1 and are functionally impaired. *Blood*. 2009;114:1537–1544.
30. O'Hear C, Heiber JF, Schubert I, et al. Anti-CD33 chimeric antigen receptor targeting of acute myeloid leukemia. *Haematologica*. 2015;100:336–344.
31. Wang QS, Wang Y, Lv HY, et al. Treatment of CD33-directed chimeric antigen receptor-modified T cells in one patient with relapsed and refractory acute myeloid leukemia. *Mol Ther*. 2015;23:184–191.
32. Marin V, Pizzitola I, Agostoni V, et al. Cytokine-induced killer cells for cell therapy of acute myeloid leukemia: improvement of their immune activity by expression of CD33-specific chimeric receptors. *Haematologica*. 2010;95:2144–2152.
33. Butler MO, Hirano N. Human cell-based artificial antigen-presenting cells for cancer immunotherapy. *Immunol Rev*. 2014;257:191–209.
34. Cieri N, Camisa B, Cocchiarella F, et al. IL-7 and IL-15 instruct the generation of human memory stem T cells from naive precursors. *Blood*. 2013;121:573–584.
35. Xu Y, Zhang M, Ramos CA, et al. Closely related T-memory stem cells correlate with in vivo expansion of CAR-CD19-T cells and are preserved by IL-7 and IL-15. *Blood*. 2014;123:3750–3759.
36. Bukczynski J, Wen T, Ellefsen K, et al. Costimulatory ligand 4-1BBL (CD137L) as an efficient adjuvant for human antiviral cytotoxic T cell responses. *Proc Natl Acad Sci U S A*. 2004;101:1291–1296.
37. Sukumar M, Liu J, Ji Y, et al. Inhibiting glycolytic metabolism enhances CD8+ T cell memory and antitumor function. *J Clin Invest*. 2013;123:4479–4488.
38. Kawalekar OU, Connor RS, Fraietta JA, et al. Distinct signaling of coreceptors regulates specific metabolism pathways and impacts memory development in CAR T cells. *Immunity*. 2016;44:380–390.
39. Le Dieu R, Taussig DC, Ramsay AG, et al. Peripheral blood T cells in acute myeloid leukemia (AML) patients at diagnosis have abnormal phenotype and genotype and form defective immune synapses with AML blasts. *Blood*. 2009;114:3909–3916.